Morphology and composition of layered anodic films on InP

F. ECHEVERRIA
Corrosion and Protection Centre, University of Manchester Institute of Science and Technology, P.O. Box 88, Manchester M60 1QD, UK

P. SKELDON
Corrosion and Protection Centre, University of Manchester Institute of Science and Technology, P.O. Box 88, Manchester M60 1QD, UK
E-mail: p.skeldon@umist.ac.uk

G. E. THOMPSON
Corrosion and Protection Centre, University of Manchester Institute of Science and Technology, P.O. Box 88, Manchester M60 1QD, UK

H. HABAZAKI
Institute for Materials Research, Tohoku University, 2-1-1 Katahira, Aoba-Ku, Sendai 980-77, Japan

K. SHIMIZU
University Chemical Laboratory, Keio University, 4-1-1 Hiyoshi, Yokohama 223, Japan

The composition and morphology of the double-layered anodic film formed at 5 mA cm^{-2} on InP in aqueous sodium tungstate electrolyte is examined by transmission electron microscopy (TEM), atomic force microscopy (AFM), Rutherford backscattering spectroscopy and nuclear reaction analysis. The outer layer is composed mainly of In_2O_3 of relatively low atomic density, about 50% that of crystalline In_2O_3. The low density is probably due partly to the presence of numerous cavities in the layer, revealed by TEM and AFM. The inner layer is enriched in phosphorus relative to the composition of the substrate, with a P : In atomic ratio of about 2.17. From the measured ratio of phosphorus to indium, the composition of the inner layer can be expressed as either $In_2O_3.2.17P_2O_5$ or $In(PO_3)_{2.17}$. The average nm V^{-1} ratio is 1.99 ± 0.07. However, there are wide variations of the local film thickness, associated with roughness at the substrate/film and film/electrolyte interfaces and local variability in the ionic current density due to cavities in the film. The film forms with a small loss of indium species to the electrolyte. The outer layer represents about 32% of the total thickness of a film formed at 100% efficiency.

1. Introduction

Optical communications and high-speed electronic systems use III-V semiconductor devices [1]. Devices using InP include metal-insulator-semiconductor field effect transistors (MISFETS), photo-electrochemical solar cells [2], light emitting diodes [1], high performance radiation-resistant space solar cells [3, 4], microwave FETS and components for optical fibre communications [5]. For the manufacture of such devices, there is interest in anodic oxidation of InP to produce thin insulating films. The following reviews briefly available information on anodizing of InP.

Study of anodizing InP in AGW electrolyte of pH 2 revealed a single-layered anodic film enriched in P_2O_5 [6]. The film formed at pH 3 was double-layered, with an outer layer composed of either In_2O_3 or $In(OH)_3$ and an inner layer containing similar amounts of indium and phosphorus [6]. The transition from single-layered to double-layered films is due to the greatly increased solubility of In_2O_3 at pH <2.5 [7]. X-ray photoelectron spectroscopy (XPS) suggested polyphosphate compounds, rather than either In_2O_3 and P_2O_5 or $InPO_4$, in the inner film material [8]. In contrast to previous films, the film formed in 0.1 *N* KOH was reported to consist mainly of In_2O_3, with some P_2O_5; the In : P ratio, determined from Auger electron spectroscopy and XPS, increased between the InP/oxide and oxide/electrolyte interfaces [9]. Anodizing in KOH of pH 6.5 resulted in nearly equal amounts of indium and phosphorus in the film [10]. The distributions of indium and phosphorus depended upon the film thickness, with a two-layered film at 33.3 nm thickness. The outer layer contained In_2O_3, with P_2O_5 present in underlying material. A Rutherford backscattering

spectroscopy (RBS) study of the film grown in *N*-methylacetamide : NH_4OH : H_2O of pH 12 disclosed an outer layer of In_2O_3 and an inner layer of P_2O_5 containing about 20% In_2O_3 [11].

XPS studies of films grown in electrolytes of various compositions and pH revealed $InPO_4$ as the main compound formed at low pH, rather than In_2O_3 and P_2O_5 [12, 13]. $In(OH)_3$, rather than In_2O_3, was present at the surface of double-layered films formed at higher pH, with an inner layer of $In(PO_3)_y$, with y in the range 2.5–4.5. A further study also suggested formation of polyphosphate, with y in the range 2–4, rather than In_2O_3, P_2O_5 or $InPO_4$ [14]. Other workers proposed the presence of $In(PO_x)_y$, with x approximately equal to 3 and y in the range 3–5 [15]. XPS depth profiling indicated $In(OH)_3$ is only present at the surface of the indium-rich layer, which was composed mainly of In_2O_3 [15]. The studies of polyphosphate formation suggest a dependence of y upon anodizing conditions [12, 14, 15]. The presence of polyphosphate enhanced the electrical properties, in particular increased resistivity and energy band gap, and physicochemical properties, including stability, of the film [14]. A composition approaching stoichiometric $In(PO_3)_3$ correlated with a reduced density of interfacial states [15].

XPS study revealed sharp film/InP interfaces, which are In-rich and P-rich following growth of films in the dark and under strong illumination, respectively [4]. However, interfaces may also be of stoichiometric composition, with In/P ratio of $\sim$1 [4, 9, 16]. Reflection electron diffraction suggests polycrystalline films [17], while reflection high energy electron diffraction indicates amorphous structures of as-grown films [12]. Heat treatment can produce weak diffraction patterns due to transformation of the indium-rich layer, with the inner layer remaining amorphous [12].

The various studies considered previously indicate that double-layered films form under conditions where In_2O_3 is stable. The outer layer consists of In_2O_3, with $In(OH)_3$ at the surface probably due to hydration. The composition of the inner layer is less certain, with proposals of In_2O_3 and P_2O_5, $InPO_4$ and $In(PO_x)_y$, with $x \sim 3$ and y in the range 2–5. The present study combines for the first time examination of cross-sections of films formed on InP in aqueous sodium tungstate electrolyte, using transmission electron microscopy (TEM) and atomic force microscopy (AFM), with analyses of compositions by RBS, in order to increase understanding of the mechanism of film growth.

2. Experimental

2.1. Specimen preparation

Specimens of *n*-type, (100) single crystal, 99.99% InP, doped with 5×10^{18} S cm^{-3}, were anodized at 5 mA cm^{-2} in aqueous 0.1 M sodium tungstate ($Na_2WO_4.2H_2O$) electrolyte (pH 8.2) at 293 K. The specimens were cleaned in acetone before anodizing and rinsed briefly in deionized water after anodizing. The anodizing was carried out in a glass cell with an aluminium counter electrode. The cell contained approximately 250 ml of electrolyte, which was stirred continuously during anodizing. The voltage-time responses were recorded during film growth.

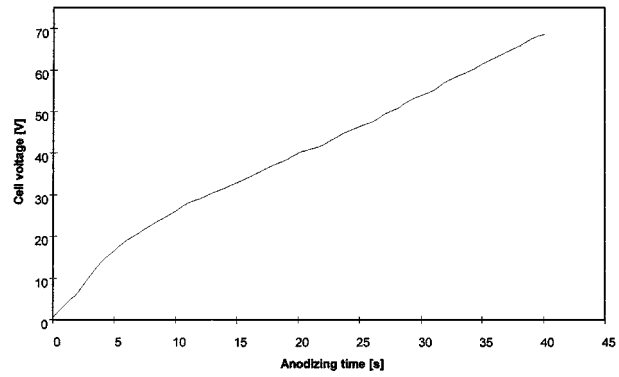

Figure 1 Voltage-time response for anodizing InP at 5 mA cm^{-2} in 0.1 M sodium tungstate electrolyte at 293 K.

2.2. Specimen examination

Specimens were sectioned by ultramicrotomy for examination by either analytical TEM [17] or AFM [18] employing JEOL FX 2000 II and Nanoscope III MultiMode instruments respectively. The films were analysed by RBS using 2.0 MeV alpha particles supplied by the 2.5 MeV Van de Graaff accelerator of the University of Paris, with interpretation of data by the RUMP program [19]. The oxygen content of the film was determined by NRA, using 830 keV deuterons [20].

3. Results

3.1. Voltage-time response

Following a voltage surge of about 0.6 V, probably due to a pre-existing film on the surface of the specimen, the response reveals immediately an approximately linear region of slope 3.1 ± 0.5 V s^{-1} to about 18 V (Fig. 1). The slope then decreases gradually to 1.4 ± 0.3 V s^{-1} by about 23 V and subsequently remains approximately constant to the termination of anodizing at 68 V. The decrease in slope occurs during anodizing InP in a range of current densities, electrolytes and conditions of illumination [4, 15, 21, 22]. It is possibly due to a phosphate/polyphosphate transformation [15]. The charge passed during anodising is 0.20 ± 0.02 C cm^{-2}. The error in the charge is associated mainly with the accuracy of the area measurement for the relatively small irregular shaped specimens. Attempts to grow relatively thick films in either 2 mM sodium tungstate electrolyte (pH 7.1), at 5 mA cm^{-2}, or the 0.1 M electrolyte, at 1 mA cm^{-2}, were unsuccessful. The voltage increased approximately linearly to about 12–14 V then approached an almost constant value of about 15 V. Others have found similar responses [4].

3.2. Transmission electron microscopy

Transmission electron micrographs of ultramicrotomed sections, about 30 nm thick, of InP anodized to 68 V disclose a double-layered film of non-uniform thickness (Fig. 2). The length of sections is limited to about 150 nm, due to fragmentation of the material during

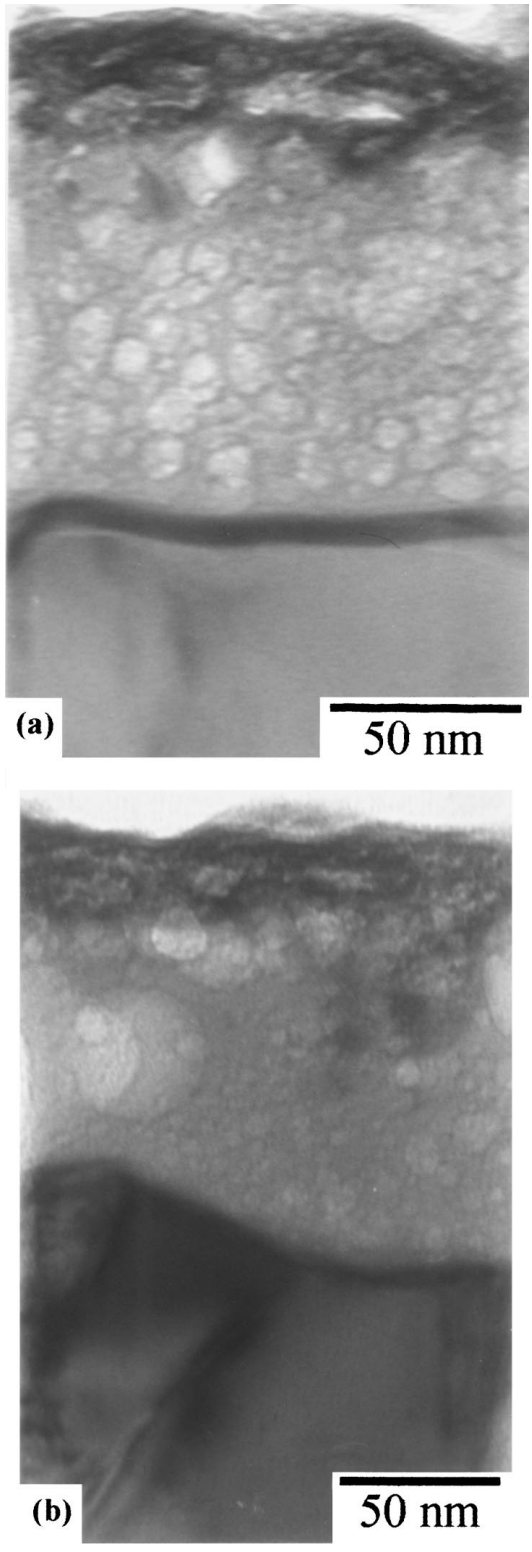

Figure 2 Transmission electron micrographs showing ultramicrotomed sections of InP anodized at 5 mA cm^{-2} to 68 V in 0.1 M sodium tungstate electrolyte at 293 K. (a) and (b) are of different regions of film and disclose the variation of film thickness across the surface of the substrate.

ultramicrotomy. The thickness of the film ranges between 102 nm and 147 nm in the examined sections. The average thickness is estimated as 135 ± 5 nm, indicating a nm V^{-1} ratio of 1.99. In previous studies, reported ratios range from 1.4 to 2.9 [21, 23, 24]. The non-uniform film thickness is associated with roughness of both the substrate/film and film/electrolyte interfaces. The outer layer, which is darker than the inner layer, is also of non-uniform thickness. The average thickness of the outer layer is 35 ± 5 nm. The ratio of the thickness of the outer layer to the thickness of the whole film is 0.26 ± 0.04. Exposure to the electron beam during TEM damages rapidly the material of the inner layer, resulting in the pore-like texture of the material. The origin of light regions, with the appearances of cavities, in the outer layer is unclear from TEM, as they are evident immediately upon observation of the section.

Energy dispersive X-ray (EDX) analysis, using a probe of approximately 20 nm diameter, reveals an indium-rich outer layer and a phosphorus-rich inner layer (Fig. 3). The low signal from phosphorus in the outer layer is almost certainly due to overlap of the beam onto the inner layer material. Analysis of the outer layer reveals the presence of a low concentration of tungsten, with signals at 8.398 and 9.673 keV. The signal ascribed to tungsten at 1.775 keV is due partly to silicon contamination of the copper grid. The amounts of indium and phosphorus in the substrate are 50 ± 1 at.%.

3.3. Atomic force microscopy

Three-dimensional images of the InP surface before anodizing reveal a relatively rough surface remaining from the commercial surface treatment of the crystal (Fig. 4a). Two main features are evident. Large depressions, about 500 nm across and 7 nm depth, occupy about 20% of the surface. Between these, the surface is decorated with fine undulations, with depth about 3 nm and with lateral dimensions about 100 nm. The plan view of regions between the main depressions suggests a cellular texture (Fig. 4b). The plan view of the anodized surface discloses a granular appearance, with features of typically a few tens of nanometres size (Fig. 4c).

Cross-sectional AFM confirms the non-uniformity of the film indicated previously by TEM, with roughness evident at the substrate/film and film/electrolyte interfaces and regions of locally thick film (Fig. 5a). The cross-sectional AFM images encompass long lengths of film, to several microns, compared with the TEM images of film fragments. The average thickness of the film is 140 ± 10 nm, which is similar to the result from TEM. Increased resolution imaging reveals the double-layered nature of the film and the fine-scale roughness of the main interfaces (Fig. 5b). The outer layer is 28 ± 6 nm thick, and the ratio of its thickness to that of the complete film is 0.20 ± 0.04, which agree with the values from TEM.

The cross-sectional images disclose fine defects, with typical dimensions about 10 nm, in the outer layer of the film, reminiscent of the light features in transmission electron micrographs. Larger defects, with typical dimensions about 50 nm, are evident in the inner layer material, mainly in the middle of the film and towards the substrate/film interface.

3.4. Rutherford backscattering spectroscopy and nuclear reaction analysis

The experimental and simulated RBS spectra reveal a double-layered film (Fig. 6). The indium-rich surface

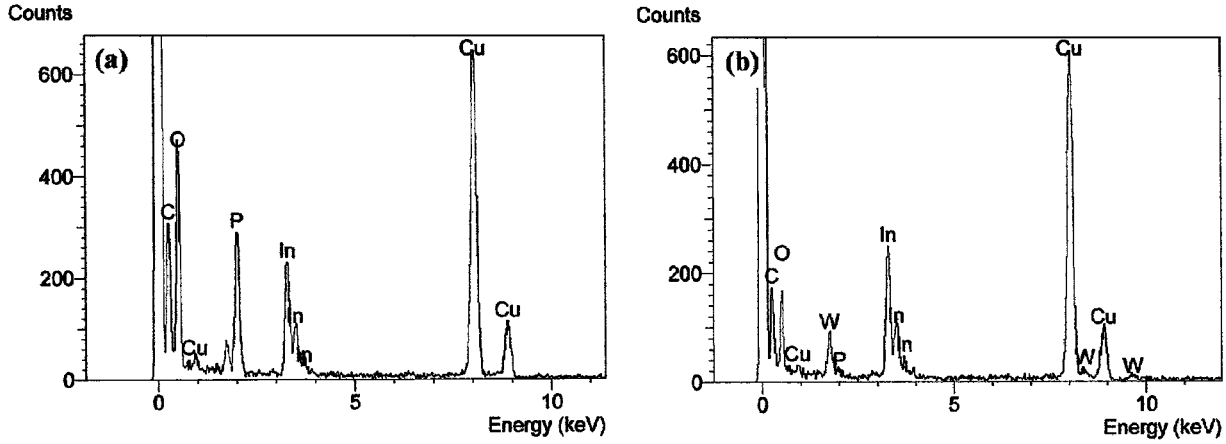

Figure 3 EDX spectra for (a) the inner and (b) the outer layer of the film formed on InP at 5 mA cm^{-2} to 68 V in 0.1 M sodium tungstate electrolyte at 293 K.

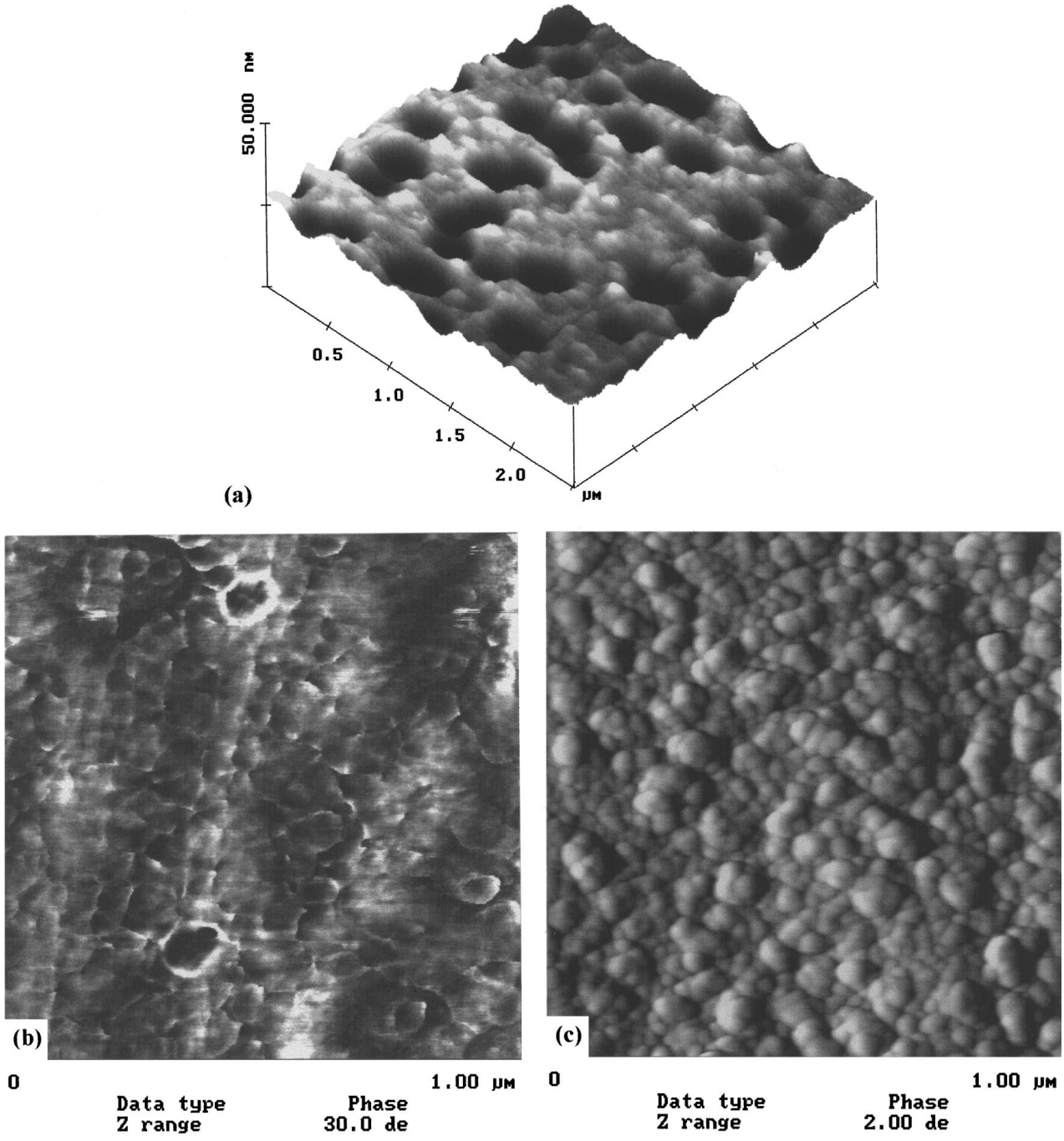

Figure 4 AFM images showing the surface of InP. (a) Three-dimensional image of the surface before anodizing. (b) Plan view, phase image of the surface before anodizing. (c) Plan view, phase image of the surface after anodizing at 5 mA cm^{-2} to 68 V in 0.1 M sodium tungstate electrolyte at 293 K.

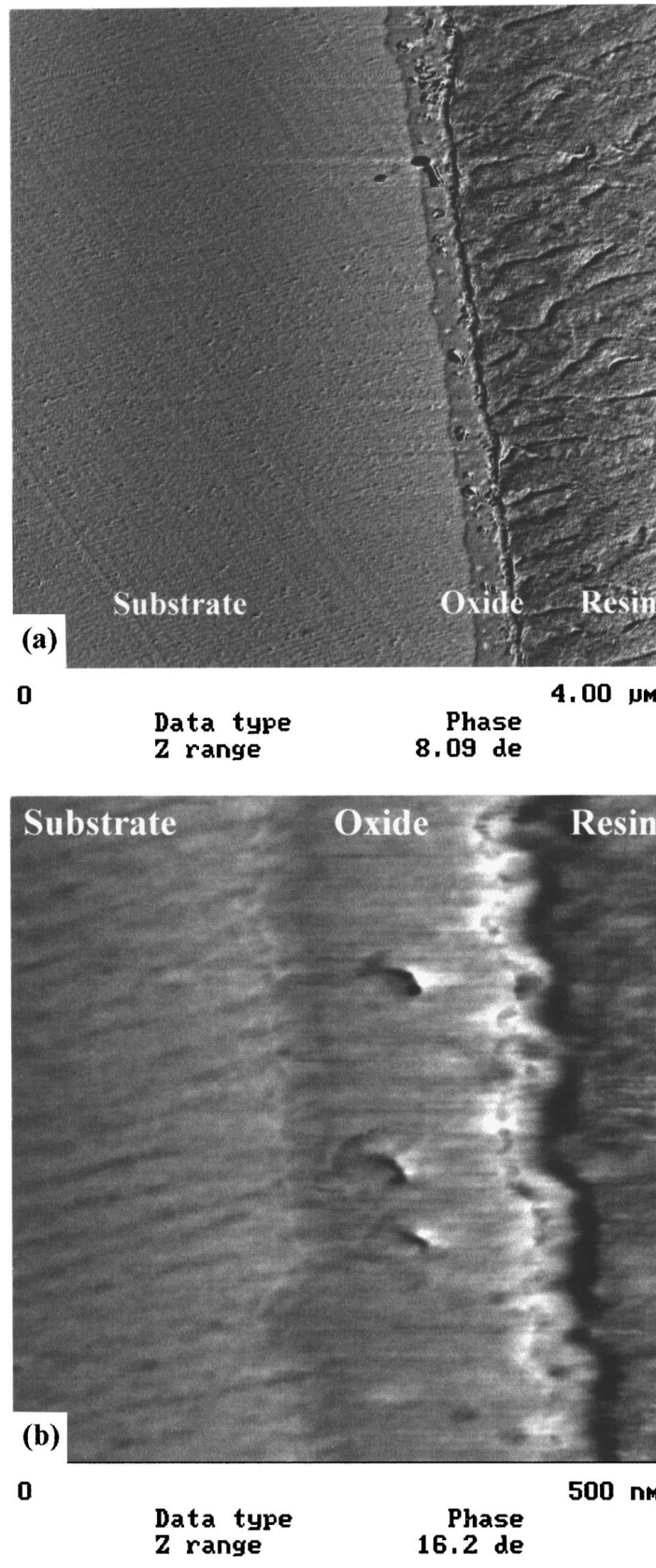

Figure 5 (a) Cross-sectional AFM phase image of InP anodized at 5 mA cm^{-2} to 68 V in 0.1 M sodium tungstate electrolyte at 293 K. (b) A phase image at increased magnification.

layer, which contains tungsten, results in distinct peaks for indium and tungsten. Phosphorus is present in the inner layer. The results of the simulation (Table I) indicate an outer layer of In_2O_3 and an inner layer with an atomic ratio of P : In of 2.17. The accuracy of the RBS results is about 5%. The tungsten is assigned to the outer layer. However, there are probably contributions from gel material and adsorbed tungstate anions at the film surface. The atomic density of indium in the outer layer of the film, calculated from the number of indium atoms from RBS and the thickness of the layer from TEM, is about 1.46×10^{22} cm^{-3}, which is low compared with

TABLE I Results of RBS analysis of InP anodized at 5 mA cm^{-2} to 68 V in 0.1 M sodium tungstate electrolyte at 293 K

Outer layer (composition)	Outer layer (In atoms cm^{-2})	Outer layer (W atoms cm^{-2})	Inner layer (composition)	Inner layer (In atoms cm^{-2})
In_2O_3	5.1×10^{16}	4.2×10^{15}	$In_2O_3.2.17P_2O_5$	5.9×10^{16}

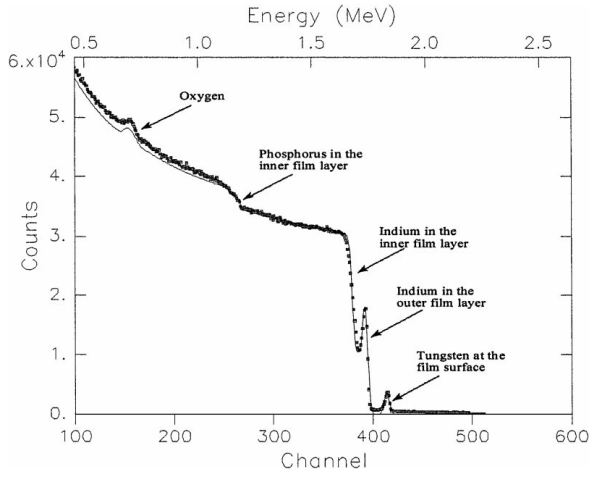

Figure 6 Experimental and simulated (solid line) RBS spectra for InP anodized at 5 mA cm^{-2} to 68 V in 0.1 M sodium tungstate electrolyte at 293 K.

that of crystalline In_2O_3, about 3.1×10^{22} cm^{-3}. The atomic density of indium and phosphorus in the inner layer is about 1.23×10^{22} cm^{-3}.

The total amounts of indium and phosphorus in the film, to an accuracy of about 5% are 1.10×10^{17} and 1.28×10^{17} atoms cm^{-2} respectively. Thus, the P : In ratio is about 1.16, suggesting the loss of about 1.8×10^{16} In atoms cm^{-2} to the electrolyte. Assuming oxidation of indium and phosphorus to the +3 and +5 states, the charge to form the film material is approximately 0.155 C cm^{-2}. The charge due to lost indium species is about 0.009 C cm^{-2}. Thus, the total charge passed for oxidation of the InP is about 0.16 ± 0.1 C cm^{-2}. The loss of indium species accounts for about 5% of the total charge due to oxidation. The loss is equivalent to about 13 nm of In_2O_3 of the reduced ionic density (compared with crystalline In_2O_3). Thus, considering the thickness from TEM, the outer layer of a film formed at 100% efficiency is about 32% of the total thickness of the film.

The RBS analysis is not particularly suited to determination of the precise oxygen content of the film, since the relatively small yield from oxygen rests on the high background from the substrate. However, the numbers of indium and phosphorus atoms suggest an oxygen content of $4.85 \pm 0.24 \times 10^{17}$ oxygen atoms cm^{-2}, compared with $4.65 \pm 0.14 \times 10^{17}$ oxygen atoms cm^{-2} determined by NRA.

4. Discussion

The anodic films formed on InP are similar in many respects to those formed on other III-V semiconductors, such as GaP and InAs, which also produce layered, amorphous anodic films. The limited number of marker experiments for III-V semiconductors indicate that the films grow by outward migration of cations and inward migration of anions [25, 26]. The counter migration of cations and anions leads to formation of film material at both the substrate/film and film/electrolyte interfaces, which, together with co-operative ionic transport processes, appears to be a general characteristic of amorphous anodic films [23]. This form of film growth is presumed to be relevant to InP, with relatively fast migration of In^{3+} ions, relative to phosphorus species, leading to the development of the double-layered films. However, the composition of the phosphorus-rich inner layer in these films is controversial, with the suggested presence of oxide, phosphate and polyphosphate species.

If it assumed that the film is essentially composed of oxide [6], the P : In ratio, determined from RBS, suggests a composition of approximately $In_2O_3.2.17P_2O_5$ for the inner layer. The composition indicates that phosphorus is present as a cation species and that the material of the inner layer comprises primarily P_2O_5, with units of In_2O_3 incorporated into its structure. The layered film is a consequence of faster migration of In^{3+} ions relative to P^{5+} ions, which leads to the formation of the outer layer of In_2O_3. Faster migration of In^{3+} ions is consistent with the lower energy of the In^{3+}–O bond, 181 kJ mol^{-1}, relative to that of the P^{5+}–O bond, 424 kJ mol^{-1}. The differential migration enhances the concentration of phosphorus in the inner layer of the film, relative to the composition of the substrate. Hydration of the surface of the film probably occurs, as indicated in a previous study [15].

Alternatively, if it is assumed that the inner layer is composed of polyphosphate, as proposed by others [12, 14, 15]. The composition of the film is represented as approximately $In(PO_3)_{2.17}$. Either possibility is consistent with the analyses. The layering is now a consequence of outward migration of In^{3+} ions and/or inward migration of polyphosphate ions. Polyphosphate ions must form at the substrate/film interface, where phosphorus oxidizes and enters the film. Their formation requires supply of O^{2-} ions to the interface. However, supply of O^{2-} ions requires the presence of oxide species in the inner layer, which is contrary to the presumed presence only of polyphosphate.

The present films reveal a non-uniform film thickness, which may be associated partly with the roughness of the initial surface of the substrate. It may also arise from generation of flaws within the film. Evidence from TEM suggests defects are present mainly within the indium-rich layer. However, the high sensitivity to the electron beam and the fragmentation of sections hinders observations of the morphology of the inner layer over extensive regions. In contrast, the length of film accessible by cross-sectional AFM is one hundred or more times greater. Cavities appear to be present in both layers of the film, with larger cavities in the inner layer.

The cavities might represent oxygen generated by oxidation of O^{2-} ions of the film, possibly involving

reduction of cation species. Reduction of chromium (VI) species to chromium (III) species is known to occur within anodic alumina films formed in chromate electrolyte [27]. The mechanism of reduction of chromium (VI) is not known, although void-like defects have been identified in the chromium-containing region of film [28].

The charge passed in formation of the film is 0.16 ± 0.01 C cm^{-2} and 0.20 ± 0.02 C cm^{-2}, as determined from results of RBS and from the product of the current density and the time of anodising respectively. The source of the difference between the results is uncertain but may indicate an electron current. Others have suggested loss of film material occurs in the initial period of anodizing, prior to the change of slope in the voltage-time response [4]. The change in the slope of the voltage-time response during anodizing InP may also be associated with development of oxygen-filled cavities. The authors are continuing study of the oxide, with examination of the cavity regions by electron energy loss spectroscopy, which can differentiate oxygen species. Such studies should elucidate further the origins of cavities and the reason for the change in slope of the voltage-time response during anodising.

5. Conclusions

1. The amorphous film formed on InP following anodizing at 5 mA cm^{-2} in 0.1 M aqueous sodium tungstate electrolyte at 293 K consists of two layers. The outer layer is composed mainly of In_2O_3. The composition of the inner layer can be expressed as $In_2O_3.2.17P_2O_5$ or, alternatively, $In(PO_3)_{2.17}$.

2. The film forms with loss of indium species to the electrolyte. The ratio of the thickness the outer layer to the thickness of the whole film, estimated for a film formed at 100% efficiency, is about 0.32.

3. The average nm V^{-1} ratio for growth of the film is about 1.99. However, the film is of relatively non-uniform thickness. Initial roughness of the substrate may be a factor in the non-uniformity of the film. However, void-like defects are present extensively within the films, which may promote non-uniform film growth.

Acknowledgements

The authors are grateful to COLCIENCIAS (Columbia) for financial support provided to F. E. They also wish to thank Dr C. Ortega of the Groupe de Physiques des Solides, Université Pierre et Marie Curie Paris VI for assistance with RBS analyses (work partly supported by Centre National de la Recherche Scientifique (GDR 86)).

References

1. P. A. KOHL, C. WOLOWODIUK and J. F. W. OSTERMAYER, *J. Electrochem. Soc.* **130** (1983) 2288.
2. H. LI and S. PONS, *J. Electroanal. Chem.* **233** (1987) 1.
3. J. MOULOT, M. FAUR, C. GORADIA, M. GORADIA, M. FAUR, S. ALTEROVITZ and S. BAILEY, in IEEE Int. Conf. on Indium Phosphide and Rel. (1996) p. 283.
4. M. FAUR, M. FAUR, D. T. JAYNE, M. GORADIA and C. GORADIA, *Surf. Interf. Anal.* **15** (1990) 641.
5. A. GUIVARC'H, H. L'HARIDON, G. PELOUS, G. HOLLINGER and P. PERTOSA, *J. Appl. Phys.* **55** (1984) 1139.
6. D. H. LAUGHLIN and C. W. WILMSEN, *Appl. Phys. Lett.* **37** (1980) 915.
7. M. POURBAIX, "Atlas of electrochemical equilibria in aqueous solutions" (National Association of Corrosion Engineers: Houston, TX. 1974).
8. Y. ROBACH, J. JOSEPH, E. BERGIGNAT, B. COMMERE, G. HOLLINGER and P. VIKTOROVITCH, *Appl. Phys. Lett.* **49** (1986) 1281.
9. C. W. WILMSEN and R. W. KEE, *J. Vac. Sci. Technol.* **15** (1978) 1513.
10. K. M. GEIB and C. W. WILMSEN, *J. Vac. Sci. Technol.* **17** (1980) 952.
11. M. SALVI, P. N. FAVENNEC, H. L'HARIDON and G. P. PELOUS, *Thin Solid Films* **87** (1982) 13.
12. G. HOLLINGER, J. JOSEPH, Y. ROBACH, E. BERGIGNAT, B. COMMERE, P. VIKTOROVITCH and M. FROMENT, *J. Vac. Sci. Technol.* **B5** (1987) 1108.
13. G. HOLLINGER, E. BERGIGNAT, J. JOSEPH and Y. ROBACH, *J. Vac. Sci. Technol.* **A3** (1985) 2082.
14. Y. ROBACH, J. JOSEPH, E. BERGIGNAT, B. COMMERE, G. HOLLINGER and P. VIKTOROVITCH, *Appl. Phys. Lett.* **49** (1986) 1281.
15. H. ISHII, H. HASEGAWA, A. ISHII and H. OHNO, *Appl. Surf. Sci.* **41/42** (1989) 390.
16. G. S. KOROTCHENKOV and V. A. MICHAILOV, *Mater. Res. Soc. Sym. Proc.* **355** (1995) 503.
17. R. FURNEAUX, G. E. THOMPSON and G. C. WOOD, *Corros. Sci.* **18** (1978) 481.
18. F. ECHEVERRIA, P. SKELDON, G. E. THOMPSON, H. HABAZAKI and K. SHIMIZU, *J. Electrochem. Soc.* **146** (1999) 3711.
19. L. R. DOOLITTLE, *Nucl. Instrum. and Meth.* **B9** (1985) 344.
20. G. AMSEL, J. P. NADAI, C. ORTEGA, S. RIGO and J. SIEJKA, *Nucl. Instrum. Method* **149** (1978) 705.
21. A. YAMAMOTO, M. YAMAGUCHI and C. UEMURA, *J. Electrochem. Soc.* **129** (1982) 2795.
22. C. W. FISCHER and K. H. HSIEH, *J. Electrochem. Soc.* **133** (1986) 2483.
23. J. P. S. PRINGLE, *Electrochim. Acta* **25** (1980) 1423.
24. K. P. PANDE and G. G. ROBERTS, *J. Vac. Sci. Technol.* **16** (1979) 1470.
25. C. W. FISCHER and J. D. CANADAY, *J. Electrochem. Soc.* **130** (1983) 1740.
26. R. P. H. CHANG, C. C. CHANG and T. T. SHENG, *Appl. Phys. Lett.* **30** (1977) 657.
27. S. W. M. CHUNG, J. ROBINSON, G. E. THOMPSON, G. C. WOOD and H. S. ISAACS, *Phil. Mag.* **B63** (1991) 557.
28. P. SKELDON, K. SHIMIZU, G. E. THOMPSON and G. C. WOOD, *Phil. Trans. R. Soc. Lond.* **A348** (1994) 295.

Received 31 January
and accepted 3 August 2000